Electronic Supplementary Information

A quantum dot-based microRNA nanosensor for point mutation assays†

Ya-ping Zeng,[a, ‡] Guichi Zhu,[a, ‡] Xiao-yun Yang,[b, ‡] Jun Cao,[c, ‡] Zhi-liang Jing,[c] and Chun-yang Zhang[a, *]

[a] Single-Molecule Detection and Imaging Laboratory, Shenzhen Institutes of Advanced Technology, Chinese Academy of Sciences, Shenzhen 518055, China.

[b] Department of Rehabilitation Medicine, Affiliated Hospital of Guangdong Medical College, Zhanjiang 524001, China.

[c] Department of Pathology, Affiliated Hospital of Guangdong Medical College, Zhanjiang 524001, China.

[‡] These authors contributed equally.

* To whom correspondence should be addressed. E-mail: zhangcy@siat.ac.cn.

EXPERIMENTAL SECTION

Materials. The HPLC-purified miRNAs, DNA oligonucleotides, RNase-free water, and RNase inhibitor were obtained from TaKaRa Biotechnology Co., Ltd. (Dalian, China). The sequences of the oligonucleotides are listed in Table 1. The T4 RNA ligase 2, the Vent (exo-) DNA polymerase, Nb.BsmI and Nt.BstNBI nicking enzymes and their corresponding buffer solutions were purchased from New England Biolabs (Beverly, MA, USA). SYBR Green I was obtained from Xiamen Bio-Vision Biotechnology (Xiamen, China). The streptavidin-coated 605 nm emission QDs were obtained from Invitrogen Co. (Carlsbad, CA, USA). The miRNeasy FFPE Kit was purchased from Qiagen (Germany). The paraffin-embedding lung tissue samples were obtained from the Department of Pathology, Affiliated Hospital of Guangdong Medical College (Zhanjiang,

China).

Table S1. Sequences of miRNAs, linear padlock probes, and capture probe [a]

note	Sequence (5'-3')
mir-196a2T	CGG CAA CAG AAA CUG UCU GAG
mir-196a2C	CGG CAA CAG AAA CUG CCU GAG
linear padlock probe-T	*P*-**TCT GTT GCC G**GA ATG CTA ATT CGA GTC TGT TGA TAA GTA GAA TGC TA**C TCA GAC AGT T**
linear padlock probe-C	*P*-**TCT GTT GCC G**GA ATG CTA ATT CGA GTC TGT TGA TAA GTA GAA TGC TA**C TCA GGC AGT T**
capture probe	Biotin-CTA ATT CGA GTC TGT TGA TAA GTA G-Cy5

[a] The underlined letter in mir-196a2T and mir-196a2C indicates the point mutation. The boldface and underlined regions of linear padlock probes indicate the binding regions of miRNAs and the recognition sites of Nb.BsmI, respectively. The underlined region of capture probe indicates the recognition sites of Nt.BstNBI. The linear padlock probe-T and the linear padlock probe-C represent mir-196a2T-specific and mir-196a2C-specific linear padlock probes, respectively.

Ligation and PG-RCA Reactions. The ligation reaction of linear padlock probe was performed in 10 μL of reaction mixture containing 1× ligation buffer (50 mM Tris-HCl, 400 mM ATP, 2 mM $MgCl_2$, 10 mM DTT, pH 7.5), 0.2 U/μL T4 RNA ligase 2, 0.8 U/μL RNase inhibitor, 100 nM linear padlock probe, and different concentrations of miRNAs. Before the ligase and the ligation buffer were added, the linear padlock probe, miRNA and RNase free water were heated at 80 °C

for 3 min, and then slowly cooled to room temperature. After ligase and ligation buffer were added, the mixtures were incubated at 39 °C for 55 min, and then cooled on the ice immediately.

The PG-RCA reaction was performed in 10 μL of reaction solution containing 2× ThermoPol buffer (40 mM Tris-HCl, 20 mM KCl, 20 mM $(NH_4)_2SO_4$, 12 mM $MgSO_4$, 0.2% Triton X-100, pH 8.8), 400 μM dNTP, 0.8 U/μL RNase inhibitor, 0.4 U Vent (exo-) DNA polymerase, 3 U Nb.BsmI, and 1 μL of ligation products. The mixtures were incubated at 60 °C for 75 min, followed by inactivation at 80 °C for 20 min. The PG-RCA products were analyzed by 1% agarose gel electrophoresis at room temperature in 1× TAE (40 mM Tris-ethylic acid, 2 mM EDTA) with 1× loading buffer and 1× SYBR Green I as the fluorescent indicator. The images of gel electrophoresis were acquired with a Kodak Image Station 4000MM (Woodbridge, CT, USA).

Nicking and Hybridization Reactions. The nicking reaction was performed in 20 μL of reaction mixture containing 0.5× buffer 3.1 (25 mM Tris-HCl, 50 mM NaCl, 5 mM $MgCl_2$, 0.5 mM DTT, pH 7.9), 10 μL of PG-RCA products, and 1 μM capture probe at 55 °C, followed by inactivation at 80 °C for 10 min. After the reaction mixture was cooled to room temperature, 2.5 μL of 0.2 μM QDs and 10 μL of 10× incubation buffer (1M Tris-HCl, 100 mM $(NH_4)_2SO_4$, and 30 mM $MgCl_2$, pH 8.0) were added to the reaction solution with a final volume of 100 μL. The mixtures were incubated at room temperature for 10 min to make the streptavidin-coated QDs conjugate with the biotin of capture probe.

Single-Molecule Detection. Before single-molecule detection, 100 μL of reaction solution was diluted 20-fold with the buffer containing 67 mM glycine−KOH (pH 9.4), 50 μg/mL BSA, 2.5

mM $MgCl_2$, 1 mg/mL Trolox. In order to minimize the photobleaching, an oxygen-scavenging buffer (1 mg/mL glucose oxidase, 0.4 % (w/v) D-glucose, and 0.04 % mg/mL catalase) was added into the imaging buffer. The glass slides were pretreated according to the method proposed by Chan et al.[1] In single-molecule measurement, a high-numerical aperture 60× oil-immersion objective (1.45 NA, PlanApo, Olympus) equipped with an inverted Olympus IX-71 microscope (Olympus, Tokyo, Japan) were used to verify the vision firstly. The QDs were excited by a Jive 488-nm DPSS laser (Cobolt) via total internal reflection. Both the QD and the Cy5 fluorescence signals were collected by an oil immersion objective (NA 1.45, 100 ×, Olympus), and imaged onto the two halves of an Andor Ixon DU897 EMCCD with a time resolution of 50 ms. Typically, an image series of 7 sequential frames on 7 locations were acquired from a single slide. Images were obtained with Image J (version 1.48e19, Broken Symmetry Software, U.S.A.).

Data Analysis. A region of interest (ROI) with 200 × 400 pixels was selected for single molecule counting. Five subframes (frame 2 to frame 6) of the image series were selected for analysis. The Cy5 counts were obtained by calculating 5 frames with the “analyze particles” function of Image J. In order to reduce the false positive signals from the noises, the size of particles was set at 2-12 pixels. Number of spots in five frames was counted separately and summed up. For quantitative analysis, the reduction of Cy5 counts was calculated based on the equation of $N_{reduction} = N_{control} - N_{miRNA}$, where $N_{reduction}$ is the reduction of Cy5 counts, $N_{control}$ is the Cy5 counts of five frames in the absence of specific miR-196a2, and N_{miRNA} is the Cy5 counts of five frames in the presence of specific miR-196a2.

SUPPLEMENTARY RESULTS

The persistence length of single-stranded DNA (ssDNA) is ~1.6 nm or three to four bases, whereas the persistence length of dsDNA is ~50 nm or 150 bases.[2] The biotin/Cy5-labeled capture probe absorbed on the surface of streptavidin-coated QD is a 25-base ssDNA with a contour length much larger than its persistence length. Thus, the ssDNA capture probe is more flexible in solution and can form a random coiled conformation, bringing the Cy5 acceptor spatially close to the QD donor and consequently leading to an improved FRET efficiency in the QD/capture probe/Cy5 complex. In this research, we used the total internal reflection fluorescence (TIRF) microscopy for QD-based miRNA nanosensor imaging. TIRF allows for the selective excitation of fluorescent molecules within 100 nm of the coverslip.[3] Theoretically, the length between the adjacent bases in dsDNA is about 0.338 nm, and the total length of capture probe should be less than 8.45 nm due to the flexibility of ssDNA.[2] The radius of a streptavidin-coated 605 nm emission QD is about 7.5 nm.[4] According to the theoretical calculation, the largest separation distance between the coverslip and the QD donor / Cy5 acceptor should be less than 31.9 nm, which is within the excitation field of TIRF.[3]

To demonstrate the detection specificity of the proposed method, the amplification products of PG-RCA reaction in the presence of mir-196a2T-specific linear padlock probe are analyzed by 1 % agarose electrophoresis gel with SYBR Green I as the fluorescent indicator. As shown in Fig. S1, no distinct band is observed in the presence of mir-196a2C (Fig. S1, lane 1), indicating no occurrence of PG-RCA reaction. While in the presence of mir-196a2T, the mir-196a2T-specific linear padlock probe can be ligated into a circular template and initiate the PG-RCA reaction, and consequently a series of DNA bands with different molecular weight are observed (Fig. S1, lane

2).

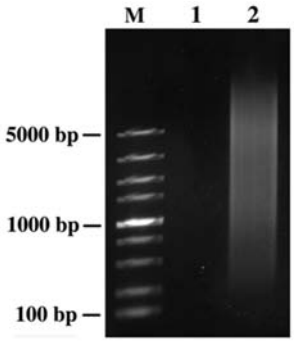

Fig. S1 Agarose gel electrophoresis analysis of the amplification products of PG-RCA reaction. Lane M is the DNA ladder marker; Lanes 1 and 2 are the amplification products in the presence of mir-196a2C and mir-196a2T, respectively.

Optimization of Experimental Condition. We investigated the influence of the capture probe-to-QD ratio on the FRET efficiency in the QD-based nanosensor and the bulk measurement, respectively. In the QD-based nanosensor, the FRET efficiency can be measured according to the equation 1.[5]

$$E = 1 - \frac{F_{DA}}{F_D} = 1 - \frac{\sum I_{DA}}{\sum I_D} \qquad (1)$$

where ΣI_{DA} is the integrated fluorescence intensities of the donor in the presence of acceptors, and ΣI_D is integrated fluorescence intensities of the donor in the absence of Cy5 acceptor. As shown in Fig. S2A, the FRET efficiency increases rapidly with the increase of capture probe-to-QD ratio from 1 to 48, and levels off beyond the ratio of 48 (Fig. S2A, red line). Additionally, we noted that the Cy5 counts have a linear relationship with the capture probe-to-QD ratio in the range from 1 to 48 (Fig. S2A, blue line). In theory, each QD can conjugate 12-15 streptavidins, and each streptavidin has three available binding sites for biotin,

thus 36-45 biotin/Cy5-labeled capture probes can be captured by a single QD.[6] The saturation capture probe-to-QD ratio of 48 obtained experimentally is close to the theoretical calculation of 36-45. The minor variance between the experimental result and the theoretical calculation might be attributed to the difference in the synthesis of streptavidin-coated QD from batch to batch.

In the bulk measurement, the FRET efficiency can be measured according to equation 2.[7]

$$E = 1 - \frac{F_{DA}}{F_D} \qquad (2)$$

Where F_{DA} is the fluorescence intensity of QD in the presence of the Cy5 acceptor, and F_D is the fluorescence intensity of QD donor alone in the absence of Cy5 acceptor. As shown in Fig. S2B, both the FRET efficiency (Fig. S2B, red line) and Cy5 fluorescence intensity (Fig. S2B, blue line) increase with the increase of capture probe-to-QD ratio from 1 to 48. When the capture probe-to-QD ratio is beyond 48, the FRET efficiency reaches a maximum value, but the Cy5 fluorescence intensity begins to decreases. It should be noted that the Cy5 counts increase and reach a plateau beyond the capture probe-to-QD ratio of 48 in the QD-based nanosensor (Fig. S2A, blue line), but the Cy5 fluorescence intensity decreases beyond the capture probe-to-QD ratio of 48 in the bulk measurement (Fig. S2B, blue line). This difference may be attributed to both the quenching of QD donor by the excess Cy5 and the inner-filter effect in the bulk measurement.[8] Thus, the capture probe-to-QD ratio obtained by the QD-based nanosensor is more accurate than that obtained in the bulk measurement, and the capture probe-to-QD ratio of 48:1 is used in the following research.

To ensure the good cleavage performance of Nt.BstNBI nicking enzyme, we further investigated the influence of reaction time upon the Cy5 counts. As shown in Fig. S2C, in the presence of mir-196a2T (Fig. S2C, red line), the Cy5 counts decrease rapidly with the increase of

reaction time from 30 min to 120 min, but no obvious change is observed beyond the reaction time of 120 min. Therefore, the reaction time of 120 min was used in the following research. It should be noted that the Cy5 counts remain unchanged even after 150 min in the presence of mir-196a2C (Fig. S2C, blue line) due to the absence of PG-RCA reaction.

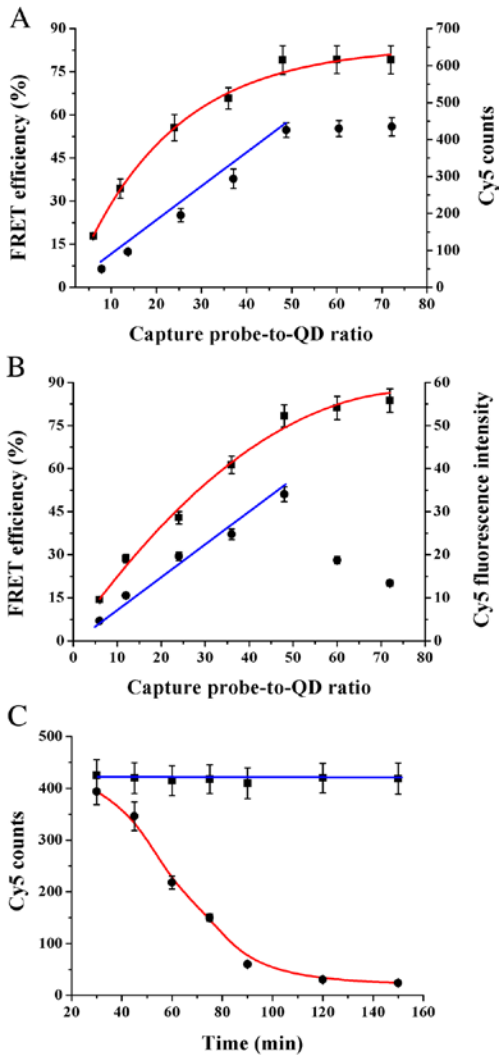

Fig. S2 (A) Variance of FRET efficiency (■) and Cy5 (●) counts as a function of the capture probe-to-QD ratio in the QD-based miRNA nanosensor. (B) Variance of FRET efficiency (■) and Cy5 (●) fluorescence intensity as a function of the capture probe-to-QD ratio in the bulk measurement. (C) Variance of Cy5 counts as a function of reaction time in the presence of

mir-196a2C (■) and mir-196a2T (●). Error bars show the standard deviation of three experiments.

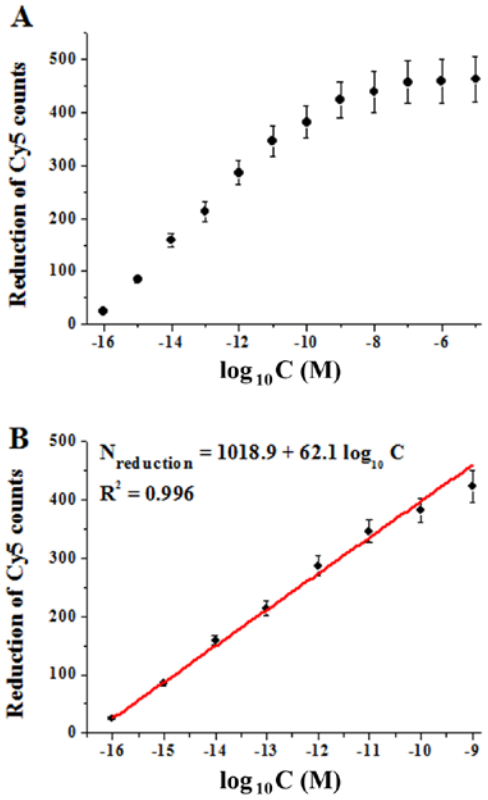

Fig. S3 (A) Variance of the reduction of Cy5 counts as a function of mir-196a2T concentration. (B) The reduction of Cy5 counts has a linear correlation with the logarithm of mir-196a2T concentration in the range from 0.1 fM to 1 nM. Error bars show the standard deviation of three experiments.

Measurement of Variant Frequency. To evaluate the capability of QD-based miRNA nanosensor for point mutation assay, we measured the artificial mixtures of mir-196a2T and mir-196a2C at various ratios of 0.001:99.999, 0.01:99.99, 0.05:99.95, 0.5:99.5, 25:75, and 100:0, respectively. The total concentration of mir-196a2T and mir-196a2C is 10 pM. As shown in Fig. S4A, the

reduction of Cy5 counts increases with the increased ratio of mir-196a2T to mir-196a2C (i.e. the input variant frequency) in the mixture. Notably, the proposed method can even distinguish as low as 0.001 % variant frequency, which is superior to most currently used approaches for miRNA point mutation assay, such as the exponential isothermal amplification-based method (0.6 %),[9] and the locked nucleic acid modified primer-based real-time PCR method (20 %).[10] The measured variant frequency is calculated as the quantity of mir-196a2T measured by the proposed method divided by the total concentration of mir-196a2T and mir-196a2C. As shown in Fig. S4B, the measured variant frequency and input variant frequency have a good linear relationship with a correlation coefficient of 0.999.

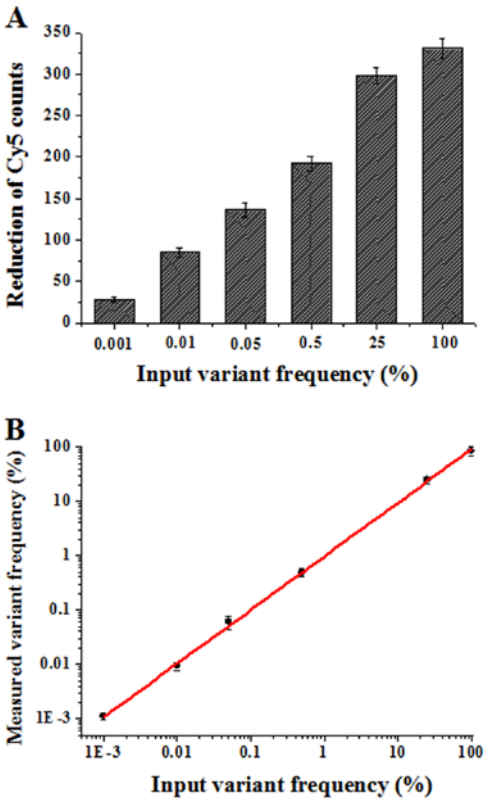

Fig. S4 (A) Variance of the reduction of Cy5 counts as a function of input variant frequency. (B) Correlation of the measured and the input variant frequency in the artificial mixtures of

mir-196a2T and mir-196a2C. Error bars show the standard deviation of three experiments.

REFERENCES

(1) H. M. Chan, L. S. Chan, R. N. S. Wong, H. W. Li, *Anal. Chem.* 2010, **82**, 6911.

(2) M. Sibgh-Zocchi, S. Dixit, V. Ivanov, G. Zocchi, *Proc. Natl. Acad. Sci. USA* 2003, **100**, 7605.

(3) A. L. Mattheyses, S. M. Simon, J. Z. Rappoport, *J. Cell. Sci.* 2010, **123**, 3621.

(4) C. Y. Zhang, H. C. Yeh, M. T. Kuroki, T. H. Wang, *Nat. Mater.* 2005, **4**, 826.

(5) A. R. Clapp, I. L. Medintz, J. M. Mauro, B. R. Fisher, M. G. Bawendi, H. Mattoussi, *J. Am. Chem. Soc.* 2004, **126**, 301.

(6) C. Y. Zhang, L. W. Johnson, *J. Am. Chem. Soc.* 2006, **128**, 5324.

(7) C. Y. Zhang, L. W. Johnson, *Anal. Chem.* 2006, **78**, 5532.

(8) P. A. Porta, H. D. Summers, *J. Biomed. Opt.* 2005, **10**, 034001.

(9) H. Jia, Z. Li, C. Liu, Y. Cheng, *Angew. Chem., Int. Ed.* 2010, **49**, 5498.

(10) L. A. Neely, S. Patel, J. Garver, M. Gallo, M. Hackett, S. McLaughlin, M. Nadel, J. Harris, S. Gullans, J. Rooke, *Nat. Methods* 2006, **3**, 41.